Conf-8708117--1

CONF-8708117--1

DE87 013548

SANS FROM POLYMERS AND COLLOIDS

John B. Hayter
Solid State Division
Oak Ridge National Laboratory
P.O. Box X
Oak Ridge, TN 37831-6031
USA

DISCLAIMER

MASTER

SANS FROM POLYMERS AND COLLOIDS

John B. Hayter
Solid State Division
Oak Ridge National Laboratory
P.O. Box X, Oak Ridge, TN 37831-6031, USA

Abstract

Small-angle neutron scattering (SANS) has been remarkably successful in providing detailed quantitative structural information on complex everyday materials, such as polymers and colloids, which are often of considerable industrial as well as academic interest. This paper reviews some recent SANS experiments on polymers and colloids, including ferrofluids, and discusses the use of these apparently complex systems as general physical models of the liquid or solid state.

1. Introduction

All too often, complex, real materials are replaced in the laboratory by simpler model systems, which may be idealised to the point where the interesting macroscopic properties which led to a study of the original material have in fact been lost. Polymers and colloids, in particular, provide examples where detailed information at the atomic level would overwhelm the experimentalist, simply because of the vast numbers of atoms involved in the most basic unit of any polymeric or colloidal material, where highly correlated atomic configurations may extend over distances from a few nanometres to a few micrometres. The problem of understanding structures of this type in real materials has become highly pressing, as more and more control is required at the sub-micron level in the so-called "nanofacturing" (or nanometre scale fabrication) of new materials and devices. The need for sub-micron, but supramolecular, information is ubiquitous in fields ranging from biomedical materials to ceramics production, from magnetic devices to waste management, from optoelectronics to metal-matrix composites. In many cases, techniques such as electron (EM) or scanning tunnelling (SCM) microscopy provide adequate information, but polymers and colloids often pose intractable problems to the microscopist. In the case of polymer blends, for example, there is rarely sufficient contrast between two different macromolecules to assess the molecular configuration of each one, let alone the ensemble average required for assessment of blend compatibility. Further, many of the most interesting systems self-assemble in solution under very specific conditions of pH or ionic strength, and correlations must be studied *in situ*.

In the case of crystalline materials, X-ray and neutron diffraction have long been the main sources of structural information, neutron diffraction being of particular importance for light-atom or magnetic structures. When radiation of wavelength λ is incident at an angle θ to a set of crystal planes having a spacing d, we expect the radiation to be reflected [with a corresponding momentum transfer of $Q=(4\pi/\lambda)\sin\theta$] if the Bragg condition, $Qd = 2\pi$, is satisfied. This result is an expression of the highly rigorous Fourier

integral theorem, which may be used to write the more general result, $Q\xi = 2\pi$, as the condition for expecting radiation to be scattered by any system which contains refractive index inhomogeneities of characteristic length ξ. Thus, although almost all polymeric and colloidal materials exhibit no long range order, the presence of scattering at a given Q directly indicates the presence of a preferred physical length in the structure. The need to study structures with large characteristic dimensions (relative to atomic scale) is thus met by studying scattering at low Q. This may be obtained by operating at large values of λ, using laser light scattering, or at small values of θ, using small angle X-ray (SAXS) or neutron (SANS) scattering; the latter is usually preferred for colloid and polymer studies because of the ability to study bulk samples, and because of the ease with which the neutron scattering power may be varied by isotopic substitution, in particular hydrogen/deuterium substition (Table 1).

Element	^1H	^2H	C	N	O	Na	Al	Si	Cl	Ti
$b/10^{-15}m$	-3.74	6.67	6.65	9.36	5.81	3.63	3.45	4.15	9.58	-3.30

Table 1. Neutron scattering amplitudes, b, for some nuclei typically found in polymers and colloids. Scattering amplitude densities, B, are found by adding all the amplitudes for a given chemical unit and dividing by the partial molar volume of the unit.

At the simplest level, the type of information obtained is very "hard", in the sense that it is model-free. (It is not even necessary to know the composition of the sample!) A typical recent case is that of a quaternary oil-water surfactant-alcohol system which indirect studies (such as conductivity) had implied was a simple molecular solution; strong small angle neutron scattering at low Q immediately showed that the system was, in fact, a colloidal micro-emulsion, with a characteristic dimension of order 3 nm [1]. A more detailed understanding requires some model input, at least of the particle symmetry, but is straightforward in dilute systems. Interesting real materials, however, are rarely dilute (in the sense of no interactions between constituent particles), and many of the studies discussed below owe as much to recent theoretical progress in the statistical mechanics of disordered dense structures, as to new experimental techniques.

2. Dilute Systems

To obtain more detailed information, we need to calculate the scattered intensity, $I(\underline{Q})$, as a function of the momentum transfer vector, $\underline{Q}$. This is straightforward when the sample contains well-defined subunits, such as polymer coils, colloidal particles or micelles, provided the subunits are randomly distributed, so that there is no correlation between scattered waves from different units; this condition is met in dilute solution, for example. We define the form-factor for coherent scattering from a given subunit as

$$F(\underline{Q}) = \sum_j b_j \exp(i\underline{Q}.\underline{r}_j) \qquad (1)$$

where b_j is the scattering amplitude of the nucleus at position $\underline{r}_j$ and the sum is over all atoms in the subunit. SANS measures in a Q-range chosen to be insensitive to atomic-scale information, and it is convenient to replace the individual atomic scattering amplitudes by averages over the smallest volume likely to be of interest in the experiment, for example a functional chemical group, or even a whole molecule in large aggregate structures. Defining $B(\underline{r})$ as the mean scattering amplitude density at a point $\underline{r}$ in the subunit, and noting that in dilute solution the subunit is displacing its own volume of solvent, of mean scattering amplitude density B_s, we obtain

$$F(\underline{Q}) = \int [B(\underline{r})-B_s] \exp(i\underline{Q}.\underline{r})\, d^3r \qquad (2)$$

This local averaging is one of the most important features when using SANS to study industrial materials. A practical example is the use of a hydrocarbon fraction containing mixed chain lengths as a solvent. The scattering power of the solvent depends basically on the density of hydrocarbon, averaged over a region of order the partial molar volume. In this context it is immaterial, for example, whether neighbouring methylenes (whose nuclei act as point scatterers for neutrons) lie on the same or on different chains, when calculating the background B_s.

Many polymer latex and colloidal particles have shapes which lead to analytic evaluation of their form-factors [2-4]. Latices, for example, often have the form of spherical particles, of radius a_1, coated by an adsorbed layer, extending to a total radius a_2; for this structure

$$F(Q) = V_1(B_1-B_2)f(Qa_1) + V_2(B_2-B_s)f(Qa_2) \qquad (3)$$

where $V_k=(4\pi/3)a_k^3$, B_1 and B_2 are the respective core and shell scattering amplitude densities, and $f(x)=3j_1(x)/x$. In this particular case, only the modulus $Q=|\underline{Q}|$ matters, since the particle cannot be orientated. The difference terms of the type B_j-B_k are known as contrasts. Reference to table 1 will show that in aqueous solution, for example, mixtures of light and heavy water allow a wide range of values of B_s, without (usually) perturbing the system. It is evident from equation 3 that choosing $B_s=B_2$ will result in scattering from the core alone, while choosing $B_s=B_1$ gives purely shell scattering. This method of unambiguous determination of partial structures is the prime reason why SANS is usually preferred to SAXS in colloid and polymer studies, despite its lesser availability. The technique is known as "contrast matching", although it is strictly contrast nulling (or refractive index matching).

Note that $F(\underline{Q})$ does not generally factor into a simple product of a contrast term and a purely geometrical term, except in the case of uniform particles. Thus for uniform ellipsoids of revolution with axes (a,a,ae) and volume V,

$$F(\underline{Q}) = V(B-B_s)\, f[Qa(\sin^2\beta + e^2\cos^2\beta)^{1/2}] \qquad (4)$$

where β is the angle between $\underline{Q}$ and the long axis. In this case, the geometrical form-factor is identical to that for a uniform sphere whose size depends on the orientation of the ellipsoid relative to $\underline{Q}$. If the shape is a right cylinder of diameter 2a and length 2l,

$$F(\underline{Q}) = 2V(B-B_s)\, j_0(Ql\cos\beta)\, J_1(Qa\sin\beta)/(Qa\sin\beta) \qquad (5)$$

where β is the angle between $\underline{Q}$ and the cylinder axis; in the above, $J_1(x)$ is the first order Bessel function of the first kind, and the $j_k(x)$ are spherical Bessel functions of order k. More complicated structures may often be modelled from assemblies of these basic shapes, simply by adding the appropriately orientated form factors with phases corresponding to their relative positions.

In many of the latest experiments, the solution contains an anisotropic distribution of particle orientations, described (in the usual polar coordinates) by an orientational probability function $p(\theta,\phi)$; the observed intensity in the general case is thus

$$I(\underline{Q}) = (1/4\pi) \int_0^{2\pi} \int_0^{\pi} F^2(\underline{Q})\ p(\theta,\phi)\ \sin\theta\ d\theta\ d\phi \qquad (6)$$

where $F(\underline{Q})$ will depend appropriately on (θ,ϕ) for a given $\underline{Q}$. Equation 6 reduces to a simple angular average in isotropic solution. If the subunits are polydisperse, this result must also be averaged over size (see, e.g. [5] and references therein). The angular averaging leads to a significant loss of information. Equation 4, for example, shows that angle-averaged ellipsoids cannot be distinguished from some appropriate distribution of polydisperse spheres in an isotropic dilute solution. In the case of complete alignment of the particles, however, we may obtain certain valuable shape signatures. The high-Q limits of equation 5, for example, show that the scattered intensity envelope will decay as Q^{-2} for $\underline{Q}$ parallel to the long cylinder axis, and as Q^{-3} perpendicular to that axis. The scattering from aligned ellipsoids, on the other hand, will decay as Q^{-4} in any direction, but in different Q ranges for the parallel and perpendicular orientations. Q^{-4} scaling at high Q will also be true for <u>any</u> well-defined uniform object in the <u>angle-averaged</u> (isotropic) case [2].

2.1 SHEAR ALIGNMENT

One of the most fascinating macroscopic properties exhibited by many colloidal dispersions is non-Newtonian hydrodynamic behaviour [6]. Even in relatively dilute solutions (volume fractions of order 1%), aggregates may assemble in such a way as to dramatically alter the bulk physical properties of the solution. The essential feature of many of these aggregates is their enormous anisotropy; it is not unusual to find cylindrical aggregates with aspect ratios of 100:1 or more. Although the macroscopic phenomenology of these systems has long been investigated, basic knowledge about, for example, the flexibility (or otherwise) of such aggregates is still lacking when it comes to designing molecules to emphasise a specific feature in the bulk properties. With biochemical molecules, in particular (but far from exclusively), the aggregates may take such a wide variety of forms, depending on the solution conditions, that even shape determination has proved elusive.

A new technique which is proving invaluable in this regard is shear alignment. The sample is placed in a thin annulus between two quartz cylinders (which are transparent to cold neutrons), and the outer cylinder is rotated about its axis; the neutron beam passes through the sample perpendicular to this axis, and the SANS patterns are measured as a function of the applied shear gradient [7]. At shear rates, G, which are large compared with the rotational diffusion coefficient, D_r, full alignment of the aggregates is obtained and observation

of the shape signatures discussed above becomes possible; shear rates up to 3×10^4 s^{-1} have been achieved. Detailed analysis of the patterns as a function of the applied shear rate allows the investigation of features such as flexibility, provided the probability function $p(\theta,\phi)$ in equation 6 can be calculated. The latter is generally not possible, but for rigid cylinders, an approximate result which agrees reasonably well with experiment (figure 1) is

$$p(\theta,\phi) = \frac{(1-\cos 2\phi_0)(1 + \sin^2\theta \cos 2\phi_0)^{3/2}}{[1 - \sin^2\theta \cos 2\phi_0 \cos 2(\phi-\phi_0)]^2} \qquad (7)$$

where $2\phi_0 = \arctan(gD_r/G)$, with g of order 8. No equivalent analytic function has so far been derived for flexible rods, but some progress has been made towards identifying particular scattering symmetries with certain types of "floppy" aggregate structures [8-9].

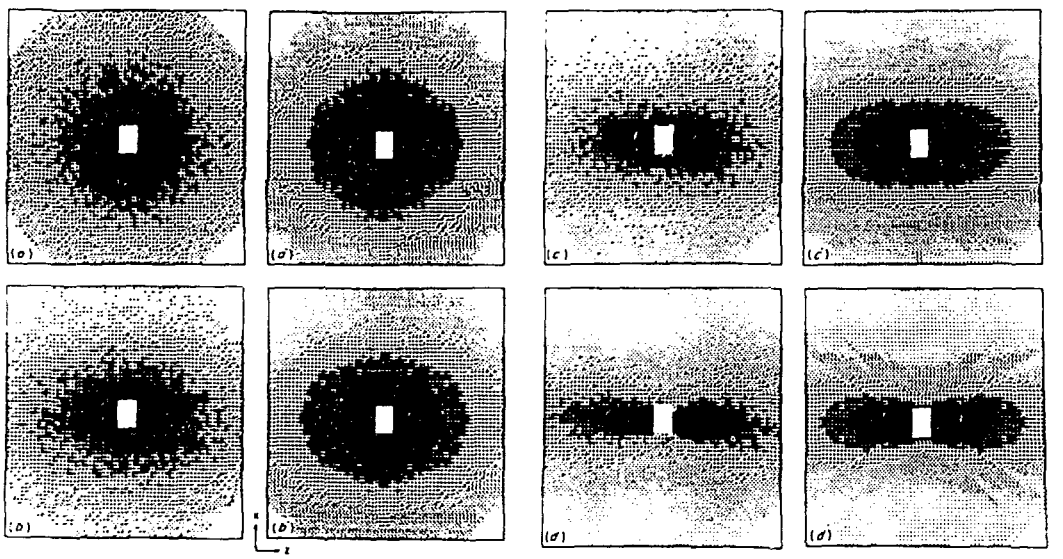

Figure 1. SANS patterns observed on a two dimensional detector for a solution of cylindrical micelles (0.03 mol. dm^{-3} hexadecyltrimethylammonium bromide in 0.4 mol. dm^{-3} KBr/D_2O) at applied shear rates (a) G=300 (b) G=1500 (c) G=3750 (d) G=7500 s^{-1}. The corresponding theoretical patterns (a')-(d') are computed from equations 5-7. Black corresponds to highest, white to lowest intensity.

2.2 FRACTAL OBJECTS

The asymptotic power-law results derived earlier for orientated solid objects may be written generally as

$$I(\underline{Q}) \propto Q^{-d-1} \qquad (8)$$

where the mass of the particle scales as r^d for $\underline{r}$ increasing in the direction of $\underline{Q}$; in the isotropic case, d is just the dimensionality of the embedding space. A more complicated situation arises when the object is not solid, but has a ramified structure, so that internal correlations within a single particle must now be taken into account. In d-dimensional space, if the mass

scales as r^D ($D<d$), the two-point density-density correlation function within the object will scale as r^{D-d}, which has the consequence

$$I(Q) \propto Q^{-D} \tag{9}$$

Structures exhibiting this type of power-law behaviour are known as fractal, and D is the Hausdorff-Besicovitch, or fractal dimension. For a single polymer chain in a Gaussian coil configuration, for example, the chain segments lie on a random walk, so that the overall coil dimension only varies as the square root of the length, and hence of the mass: D=2, and we expect $I(Q) \propto Q^{-2}$ for Q large enough to correspond to correlation lengths within the coil. The exact result for a Gaussian coil is known to be [10]

$$I(Q) \propto G(y) = [\exp(-y)+y-1]/y^2 \tag{10}$$

where $y=Q^2R_g^2$ and R_g is the radius of gyration; it is seen that the scaling result is indeed recovered at high Q.

Colloidal aggregates such as gels often exhibit fractal behaviour, with a fractal dimension which is characteristic of the kinetics of formation of the structure. In particular, diffusion limited aggregation leads to $D \approx 2.5$ in three dimensions, while cluster-cluster aggregation yields $D \approx 1.75$; in many systems, intermediate behaviour is observed. The wide Q-range over which the power-law behaviour may be observed makes this a field in which light, X-ray and neutron scattering are often used concurrently [11-12].

3. Concentrated Systems

3.1 POLYMER BLENDS

Solid polymer blends (or alloys) provide one of the most important current areas of dense polymer research. SANS has long been a unique tool for determining polymer configurations in the solid state, since single chains may be labelled for study, using deuteration to vary the contrast; an excellent review is given by Wignall [13]. In the case of a mixture of polymers, SANS is able to examine the chain configuration of each component separately at the molecular level, and to answer fundamental questions about blend compatibility at temperatures where eventual phase separation occurs too slowly to be determined easily by other techniques. The use of contrast variation presupposes that isotope effects are unimportant, and this has generally proved to be the case. Attempts to measure isotope effects have, in fact, turned out to be surprisingly difficult, but in a recent series of experiments Bates and coworkers have succeeded in demonstrating the existence of an upper critical solution temperature in binary mixtures of protonated and deuterated forms of the same polymer [14]. If N_H and N_D are the respective degrees of polymerisation of H and D polymer, in a mixture containing a volume fraction ϕ of the deuterated form, the SANS intensity is, in mean-field approximation,

$$[I(Q)]^{-1} \propto [N_D\ \phi\ G(R_D,Q)]^{-1} + [N_H\ (1-\phi)\ G(R_H,Q)]^{-1} - 2\chi_{HD} \tag{11}$$

where the function G is given by equation (10). Measurement of I(Q) thus allows determination of the Flory interaction parameter, χ_{HD}, which depends on the segment-pair interaction energy between D and H forms of the polymer; for

ideal mixing, $\chi_{HD} = 0$, whereas if χ_{HD} exceeds a critical value, χ_c, phase separation will occur. Measurements on polystyrene and polybutadiene confirm that this is indeed the case [14-15].

Although occurring at room temperature, these effects are quantum mechanical in nature [15]; they are a consequence of mass-induced changes in zero point motion, in conjunction with the anharmonicity of the interatomic potential. The effects are sufficiently subtle to be of no consequence in most contrast variation experiments, but provide an excellent introduction to the way in which polymers may be used "in reverse" as model physical systems.

3.2 COLLOIDS WITH ISOTROPIC INTERACTIONS

Most concentrated polymeric or colloidal materials exhibit strong short-range, but no long-range, order between particles. Thus, unlike the crystallographic case, where lattice symmetry permits the evaluation of sums over the entire sample (once the unit cell is known), the extension of equation 1 to concentrated systems is, in general, intractable. Even when the "unit cell" (i.e. the single particle geometry) is known, the relative particle positions can only be described in terms of a pair distribution function, $g(\underline{r})$, which gives the probability of finding a neighbour at a position $\underline{r}$ relative to a given particle; the rigorous evaluation of $g(\underline{r})$ is still an unsolved problem of statistical mechanics. Further, in the case of many self-assembling aggregates, such as micelles, the single particle size (and even symmetry) varies widely with concentration, so that the problem of determining particle geometry cannot be separated from the very difficult problem of determining the inter-particle arrangements which usually give the material its properties of interest. Despite this, remarkable progress has been made in recent years in formulating excellent approximate statistical mechanical theories for many realistic colloidal systems. The first quantitative study [16] was undertaken on a solution of charged, spherical micelles, for which the SANS intensity factors into two terms:

$$I(Q) = P(Q).S(Q) \qquad (12)$$

where $P(Q) = F^2(Q)$ is the scattering which would be observed if a single particle could be isolated (section 2), and the so-called structure factor, $S(Q)$, is the spatial Fourier transform of $g(r)$. $S(Q)$ has two important limits:

$$S(Q \to \infty) = 1 \qquad (13a)$$

$$S(Q \to 0) = nk_BT\chi_T \qquad (13b)$$

where n is the particle number density, and χ_T the osmotic compressibility of the suspension. The scattering at high Q is thus due to particle geometry alone, while at Q=0 an increase or decrease in the scattering, relative to that expected from the non-interacting particles, shows immediately whether the potential in the system is attractive or repulsive. For charged spherical colloids, an analytic structure factor [17] is available which gives sufficiently accurate results to permit in situ SANS evaluation of the surface potential on spherical colloidal particles in dense suspension (figure 2). The method is routinely used, both for determining colloidal structure and as a model technique for improving estimates of S(Q) (see [18-21] and references therein).

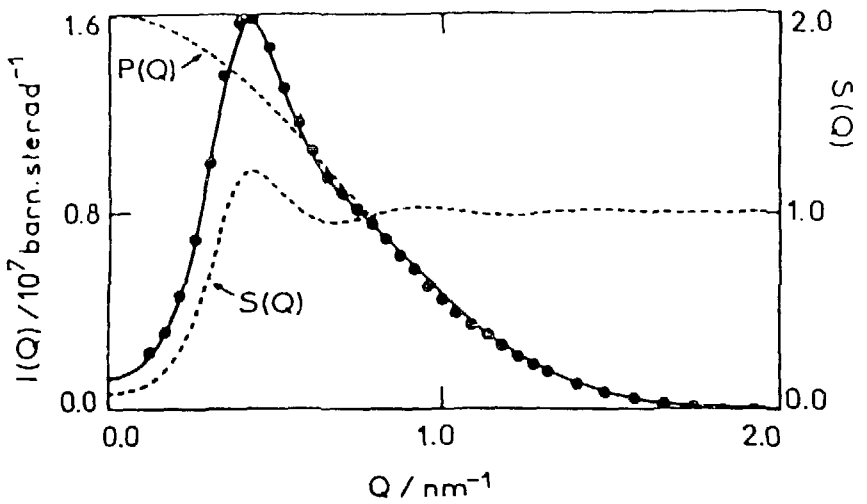

Figure 2. Measured SANS intensity (•) from a dispersion of spherical micelles (0.03 mol. dm^{-3} hexadecyltrimethylammonium chloride) which is numerically dilute, but nevertheless shows strong interaction effects. Note the suppression of forward scattering, reflecting the reduced osmotic compressibility due to charge-charge interactions between micelles. The lines correspond to equation 12, using a screened Coulomb potential to calculate S(Q) [16-18].

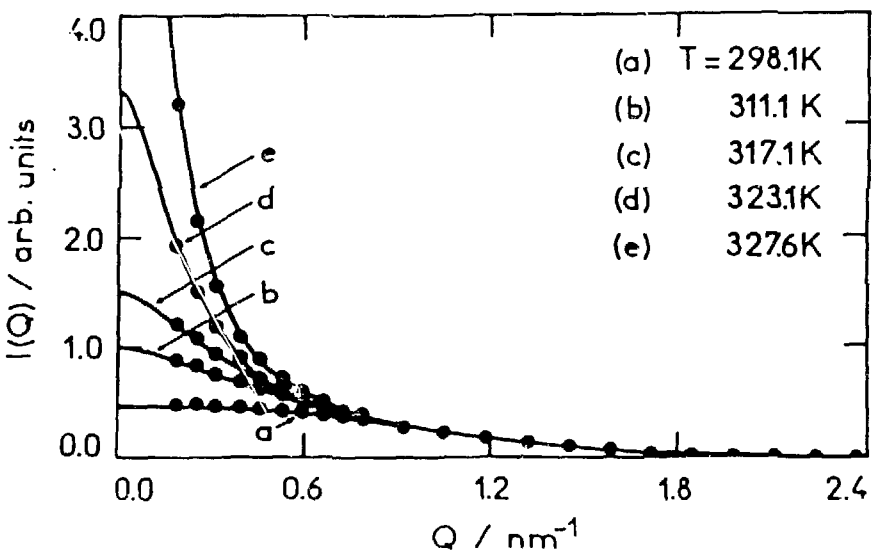

Figure 3. Measured SANS intensity (•) from a 7% solution of n-octyl pentaoxyethylene glycol monoether in D_2O as a function of temperature. Note the strong enhancement of forward scattering as the temperature approaches the lower consolution critical temperature (T_c = 329.7 K). The lines correspond to equation 12 with S(Q) computed from an attractive Yukawa potential [22].

When the inter-particle potential is attractive, equations 12 and 13b predict an increase in forward scattering. This behaviour is found, for example, with certain non-ionic micelles, in which hydrogen-bonding plays an important role (figure 3). In these systems, isotope effects may occur when H_2O/D_2O contrast variation is used, due to the change in water structure when the vibrational levels of the H-bonds are altered; it usually amounts to no more than a temperature renormalisation, however, and is easily accounted for [22-24].

3.3 COLLOIDS WITH ANISOTROPIC INTERACTIONS

For colloids which interact anisotropically because the particles are themselves anisotropic, the problem of finding a general expression analogous to equation 12 remains unsolved; even numerical techniques are of little help, since the interparticle potential cannot usually be expressed in closed analytic form. However, there are certain anisotropic cases where considerable progress has been made. The first is an extension of the shear experiments discussed in Section 2.1. If sufficient shear is applied to saturate the alignment, so that all particles are parallel, there is again a rigorous result

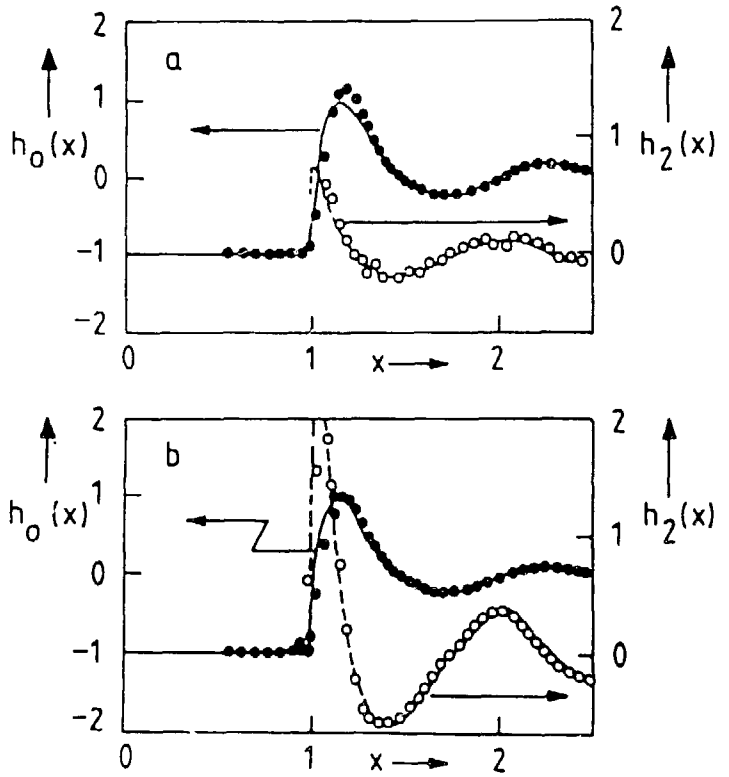

Figure 4. Central (h_0) and dipolar (h_2) terms in the total correlation function for two ferrofluids having the same (31%) volume fraction, but with different ratios of magnetic to non-magnetic material in the particle, leading to reduced moments (a) $\mu^*=2/\sqrt{3}$ (b) $\mu^*=4/\sqrt{3}$. Distance, x, is expressed in units of the total particle diameter. The lines correspond to the analytic analysis used in SANS measurements [26], while the circles are computer simulation results [27].

$$I(\underline{Q}) = P(\underline{Q}).S(\underline{Q}) \qquad (14)$$

which allows SANS measurement of the anisotropic structure factor, $S(\underline{Q})$, in aligned gels, for example [7].

A second class of important practical materials in which great progress has been made is that of magnetic colloids, or ferrofluids, in which (almost) isotropic particles interact through a central plus dipolar potential. In the presence of a saturating applied magnetic field, equation 14 again applies, with $S(\underline{Q})$ available in analytic form [25]. There is now a new feature which is unique to SANS: $P(\underline{Q})$ depends on the relative orientation of the dipole to the neutron polarisation, as well as to the direction of $\underline{Q}$. This provides, in addition to the usual contrast variation techniques, the additional power of polarisation analysis, which permits remarkably detailed information to be obtained even on industrial ferrofluids [26]. Figure 4 shows how the dipolar correlations dominate the (central) excluded volume correlations in a typical ferrofluid as the relative fraction of magnetic material in the particle increased.

4. Reverse Modelling

Once a colloidal system has been well characterised by SANS, it may often be used "in reverse" as a model physical system. The utility of this approach is that the model is a true many-body system, well beyond the scope of any realistic computer simulation, and yet key parameters of the model are still under the control of the experimentalist. An example has already been given in section 3.1; the spinodal point of the isotopic mixture

$$\chi_c = \{(N_D\ \phi)^{-1} + [N_H\ (1-\phi)]^{-1}\}/2 \qquad (15)$$

may be varied at will, since N_D, N_H and ϕ are independently variable. Another common example is provided by charged polymer latex dispersions, in which the interparticle interactions are dominated by screened Coulomb forces whose strength and range are controllable experimentally; the mean interparticle distance, relative to the range of the potential, may also be widely varied, simply by changing the amount of material (and hence the number density) in the dispersion. An appropriate choice of these parameters will cause the latex suspension to crystallise in bcc or fcc symmetry, depending on the density. These colloidal crystals provide unique models for shear melting studies at low values of applied stress (figure 5).

Ferrofluids provide an especially interesting basis for models of this type, since they may be mixed to form a completely new class of materials in the presence of a saturating applied field: binary Ising fluids. Although studies of these new liquid alloys are in their infancy [29], the problem of calculating the partial structure factors for correlations between the different components has recently been solved analytically [30] and found to agree with experiment. These materials offer fascinating possibilities for sub-micron engineering via fields and field gradients; even if one component is non-magnetic, it will nevertheless develop anisotropic correlations in the mixed fluid. SANS is especially suited to studies of these types of material, since cross-correlations in the fluid may be directly measured by using a combination of contrast variation and polarisation analysis techniques.

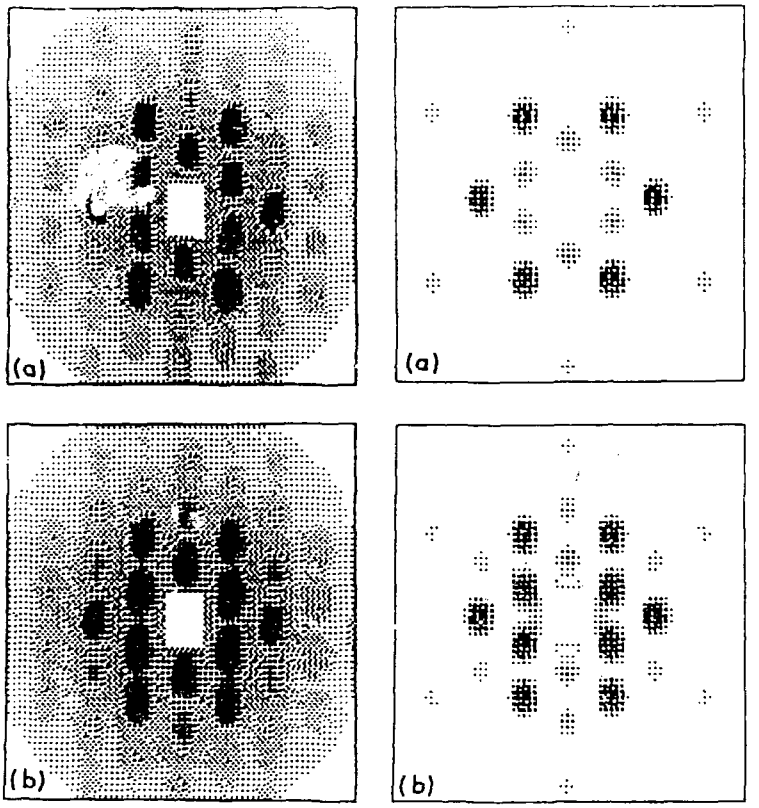

Figure 5. Two-dimensional SANS patterns for a dense, charged latex suspension used as a model system for shear-melting studies [28]. (a) Zero shear; the scattering corresponds to the (111) reflection from a face-centred cubic structure. (b) Shear rate $G=30\ s^{-1}$; note the development of strong fourfold symmetry in addition to the six-fold pattern originally present. Figures on the left are experimental results, those on the right are theoretical calculations based on a zig-zag flow model. The scale is $Q = \pm 0.1\ nm^{-1}$ in each direction.

5. Conclusion

Contrast variation, low absorption and polarisation analysis combine to make SANS a uniquely powerful tool for the study of colloidal and polymeric structures, at a resolution ideally suited to averaging over certain "industrial" aspects of real samples, while preserving information of interest. Although only elastic scattering experiments have been discussed in this paper, it is important to note that time-dependent studies are also possible at the microscopic level. Small angle neutron spin echo, in particular, has been used to study local segmental dynamics in polymers [31-34] and polyelectrolytes [35], using contrast variation in the same way as in static SANS. These techniques may also be used to study certain fundamental aspects of colloidal hydrodynamics [16,36].

Acknowledgements

This research was partially sponsored by the Division of Materials Sciences, United States Department of Energy, under contract DE-AC05-84OR21400 with Martin Marietta Energy Systems, Inc. Experiments were performed at the Institut Laue-Langevin, Grenoble, France and at the National Center for Small Angle Scattering Research, funded by National Science Foundation Grant DMR-77-244-58 through Interagency Agreement 40-637-77 with the Department of Energy.

References

1) Caponetti, E., Magid, L. J., Hayter, J. B. and Johnson, J. S.: Langmuir, 1986, 2, 722.
2) Guinier, A. and Fournet, G., "Small Angle Scattering of X-rays," Wiley, New York (1955).
3) Beeman, W. W., Kaesberg, P., Anderegg, J. W. and Webb, M. B., Handbuch der Physik, 1957, XXXII, 321.
4) Kostorz, G. in "Treatise on Materials Science," G. Kostorz, ed., Academic Press, New York (1979) Chapter V.
5) Hayter, J. B. in "Physics of Amphiphiles: Micelles, Vesicles and Microemulsions," V. Degiorgio and M. Corti, eds., North Holland, Amsterdam, (1985) p. 59.
6) Bird, R. B., Hassager, O., Armstrong, R. C. and Curtiss, C. F., "Dynamics of Polymeric Liquids," Wiley, New York (1977); see also the entire issue of Physics Today, 1984, 37(1), which is devoted to nonequilibrium fluids.
7) Hayter, J. B. and Penfold, J., J. Phys. Chem., 1984, 88, 4589.
8) Cummins, P. G., Hayter, J. B., Penfold, J. and Staples, E., J. Chem. Soc. Faraday Trans. I, in press.
9) Hayter, J. B., Rivera, M. and McGroarty, E. J., J. Biol. Chem., 1987, 262, 5100.
10) Berne, B. J. and Pecora, R., "Dynamic Light Scattering," Wiley, New York (1976) p. 168.
11) Schaefer, D. W., Martin, J. E., Wiltzius, P. and Cannell, D. S., Phys. Rev. Lett., 1984, 52, 2371.
12) Kjems, J. K., Freltoft, T., Richter, D. and Sinha, S. K., Physica 1986, 136B, 285.
13) Wignall, G. D., in "Encyclopedia of Polymer Science and Engineering," J. I. Kroschwitz, ed., Wiley, New York (1987).
14) Bates, F. S., Wignall, G. D. and Koehler, W. C., Phys. Rev. Lett., 1985, 55, 2425.
15) Bates, F. S., Dierker, S. B. and Wignall, G. D., Macromolecules, 1986, 19, 1938.
16) Hayter, J. B. and Penfold, J., J. Chem. Soc. Faraday Trans. I, 1981, 77, 1851; Molec. Phys., 1981, 42, 109.
17) Hansen, J.-P. and Hayter, J. B., Molec. Phys., 1982, 46, 651.
18) Hayter, J. B. and Penfold, J., Colloid Polymer Sci., 1983, 261, 1022.
19) Bratko, D., Friedman, H. L., Chen, S.-H. and Blum, L., Phys. Rev., 1986, A34, 2215.
20) Hayter, J. B., Hayoun, M. and Zemb, T., Colloid Polymer Sci., 1984, 262, 798.
21) Hayter, J. B. and Zemb, T., Chem. Phys. Lett., 1982, 93, 91.

22) Hayter, J. B. and Zulauf, M., Colloid Polymer Sci., 1982, 260, 1023.
23) Corti, M., Degiorgio, V., Hayter, J. B. and Zulauf, M., Chem. Phys. Lett., 1984, 109, 579.
24) Zulauf, M., Weckstroem, K., Hayter, J. B., Degiorgio, V. and Corti, M., J. Phys. Chem., 1985, 89, 3411.
25) Hayter, J. B. and Pynn, R., Phys. Rev. Lett., 1982, 49, 1103.
26) Pynn, R., Hayter, J. B. and Charles, S. W., Phys. Rev. Lett., 1983, 51, 710.
27) Hess, S., Hayter, J. B. and Pynn, R., Molec. Phys., 1984, 53, 1527.
28) Hayter, J. B., Pynn, R., Charles, S. W. and Skjeltorp, A. T., Report ORNL-6306, Oak Ridge National Laboratory (1986) p. 152.
29) Ackerson, B. J., Hayter, J. B., Clark, N. A. and Cotter, L., J. Chem. Phys., 1986, 84, 2344.
30) Hayter, J. B. and Pynn, R., to be published.
31) Richter, D., Hayter, J. B., Mezei, F. and Ewen, B., Phys. Rev. Lett., 1978, 41, 1484.
32) Nicholson, L. K., Higgins, J. S. and Hayter, J. B., Macromolecules, 1981, 14, 836.
33) Richter, D., Ewen, B. and Hayter, J. B., Phys. Rev. Lett., 1980, 45, 2121.
34) Higgins, J. S., Nicholson, L. K. and hayter, J. B., Polymer, 1981, 22, 137.
35) Hayter, J. B., Jannink, G., Brochard-Wyart, F. and de Gennes, P.-G., J. Phys. (Paris), 1980, 41, L451.
36) Hayter, J. B., Physica, 1986, 136B, 269.